



HAL
open science

Genome insights of mercury methylation among Desulfovibrio and Pseudodesulfovibrio strains

Marisol Goñi, Christophe C. Klopp, Magali Ranchou-Peyruse, Anthony Ranchou-Peyruse, Mathilde Monperrus, B.K. Hassani, Remy Guyoneaud

► **To cite this version:**

Marisol Goñi, Christophe C. Klopp, Magali Ranchou-Peyruse, Anthony Ranchou-Peyruse, Mathilde Monperrus, et al.. Genome insights of mercury methylation among Desulfovibrio and Pseudodesulfovibrio strains. *Research in Microbiology*, 2020, 171 (1), pp.3-12. 10.1016/j.resmic.2019.10.003 . hal-02390352

HAL Id: hal-02390352

<https://hal.science/hal-02390352>

Submitted on 4 Jan 2022

HAL is a multi-disciplinary open access archive for the deposit and dissemination of scientific research documents, whether they are published or not. The documents may come from teaching and research institutions in France or abroad, or from public or private research centers.

L'archive ouverte pluridisciplinaire **HAL**, est destinée au dépôt et à la diffusion de documents scientifiques de niveau recherche, publiés ou non, émanant des établissements d'enseignement et de recherche français ou étrangers, des laboratoires publics ou privés.

1

2 **Genome insights of mercury methylation among *Desulfovibrio* and *Pseudodesulfovibrio* strains**

3

4 Marisol Goni-Urriza^{a*}, Christophe Klopp^b, Magali Ranchou-Peyruse^a, Anthony Ranchou-Peyruse^a,
5 Mathilde Monperrus^c, Bahia Khalfaoui-Hassani^a, Rémy Guyoneaud^a

6

7 ^a Environmental Microbiology, CNRS/ UNIV PAU & PAYS ADOUR/ E2S UPPA, Institut des sciences
8 analytiques et de physicochimie pour l'environnement et les matériaux, IPREM, UMR5254, Pau,
9 France

10 ^b Plateforme bioinformatique Genotoul, UR875 Biométrie et Intelligence Artificielle, INRA, Castanet-
11 Tolosan, France

12 ^c CNRS/ UNIV PAU & PAYS ADOUR/ E2S UPPA, Institut des sciences analytiques et de physicochimie
13 pour l'environnement et les matériaux, IPREM, UMR5254, Anglet, France

14

15

16

17

18

19

20 marisol.goni@univ-pau.fr (*Correspondence and reprints); christophe.klopp@inra.fr;

21 magali.ranchou-peyruse@univ-pau.fr; anthony.ranchou-peyruse@univ-pau.fr;

22 mathilde.monperrus@univ-pau.fr; b.khalfaoui-hassani@univ-pau.fr; remy.guyoneaud@univ-pau.fr

23 **Abstract**

24 Mercury methylation converts inorganic mercury into the toxic methylmercury, and the
25 consequences of this transformation are worrisome for human health and the environment. This
26 process is performed by anaerobic microorganisms, such as several strains related to
27 *Pseudodesulfovibrio* and *Desulfovibrio* genera. In order to provide new insights into the molecular
28 mechanisms of mercury methylation, we performed a comparative genomic analysis on mercury
29 methylators and non-methylators from (*Pseudo*)*Desulfovibrio* strains. Our results showed that
30 (*Pseudo*)*Desulfovibrio* species are phylogenetically and metabolically distant and consequently, these
31 genera should be divided into various genera. Strains able to perform methylation are affiliated with
32 one branch of the phylogenetic tree, but, except for *hgcA* and *hgcB* genes, no other specific genetic
33 markers were found among methylating strains. *hgcA* and *hgcB* genes can be found adjacent or
34 separated, but proximity between those genes does not promote higher mercury methylation. In
35 addition, close examination of the non-methylator *Pseudodesulfovibrio piezophilus* C1TLV30 strain,
36 showed a syntenic structure that suggests a recombination event and may have led to *hgcB*
37 depletion. The genomic analyses identify also *arsR* gene coding for a putative regulator upstream
38 *hgcA*. Both genes are cotranscribed suggesting a role of ArsR in *hgcA* expression and probably a role
39 in mercury methylation.

40

41

42 **Keywords:** Sulphate reducing bacteria; phylogeny; synteny; comparative genomics; regulation

43

44 1. Introduction

45 Mercury is of global environmental and health concern. Inorganic mercury (Hg) is t able to be
46 converted into highly neurotoxic methylmercury (MeHg), which is bioaccumulated and bioamplified
47 in food webs [1]. Therefore, mercury and its derivative compounds have been placed as priority
48 pollutants by more than hundred countries that signed the United Nation Minamata convention
49 aiming to reduce the emissions and exposure to mercury. The MeHg is almost exclusively from biotic
50 origin, produced in anoxic environments principally by sulfate and iron reducers [2–5]. Mercury
51 methylation in periphyton, related to algal primary productivity, has been demonstrated to be higher
52 than in anoxic sediments [6,7], suggesting that mercury methylation could be resistant to oxygen.
53 Moreover, mercury methylation was suggested to occur via an uncultivated microaerophilic
54 bacterium (*Nitrospina*) in oxic water column [8]. Understanding the biotransformation processes of
55 Hg is a key component of risk assessment of mercury in ecosystems and human health.

56 Although MeHg production can be associated to specific microbial metabolisms (eg., sulfate
57 reducing microorganisms [2]), no phylogenetic link can be found between mercury methylating
58 microorganisms [3,4]. Among them, *Desulfovibrio* and *Pseudodesulfovibrio* strains are of interest
59 since part of them are well known methylators and others are unable to methylate mercury.
60 *Desulfovibrio* is a very large genus, including today 68 approved species and 8 subspecies, whereas
61 *Pseudodesulfovibrio*, recently described [9], includes only two approved species, previously affiliated
62 with *Desulfovibrio* [List of Prokaryotic Names with Standing in Nomenclature (LPNS)]. Both genera
63 include anaerobic bacteria able to perform sulfate respiration with a versatile metabolism and are
64 phylogenetically distant based on 16S rRNA gene sequences. Since the first strain of *Desulfovibrio*
65 isolated by Beijerinck in 1895, many *Desulfovibrio* strains have been isolated in different areas around

66 the world aiming different studies, such as for their role in global biogeochemical cycles, degradation
67 of contaminants and metals' transformations [11].

68 Genomes of 17 strains affiliated with *Desulfovibrio* and *Pseudodesulfovibrio* capable (or
69 suspected) to methylate mercury, are available. Four of them (*Pseudodesulfovibrio hydrargyri*
70 BerOc1, *Desulfovibrio desulfuricans* ND132, *Desulfovibrio africanus* strains PCS and WB) have been
71 frequently used as model strains for investigating methylation process, including the mercury species
72 distribution and isotopic fractionation [12,13], the mercury availability and uptake [14–16], the
73 genetic determinisms and the expression of genes involved in mercury methylation [17–19] , and for
74 proteome analyses [20,21]. Most importantly, *hgcA* and *hgcB* genes are the only cluster of genes
75 described as necessary for mercury methylation [17]. The *hgcA* gene encodes a putative corrinoid
76 protein, HgcA that could serve as a methyl carrier and, *hgcB* gene encodes a 2 [4Fe-4S] ferredoxin,
77 providing the electron required for corrinoid cofactor reduction. All the known mercury methylators
78 carry those genes. However, they have different methylation potentials that remain unexplained.
79 Moreover, the expression of those genes is not inducible by mercury [18,21,22], and no link have
80 been observed between their expression and methylation potentials. Thus, mercury methylation
81 appears as a complex mechanism in which the extracellular speciation of mercury [15,23–25], growth
82 behavior [26], and its concentration [21] drive significantly the process.

83 In this study, we compared *Desulfovibrio* and *Pseudodesulfovibrio* strains' genomes. We
84 particularly focused on strains able to (or suspected to) methylate mercury and we compared them
85 with those unable to perform this mechanism in order to provide new insights on cellular mercury
86 methylation process. The potential of mercury methylation of some strains showing different
87 genomic structure of genes known to be involved in mercury methylation is studied.

88

89

90 **2. Material and methods**

91 *2a. Phylogeny of Desulfovibrio genus and Desulfovibrio genomes*

92 The validated species from *Desulfovibrio* and *Pseudodesulfovibrio* genera were obtained from
93 the reference List of Prokaryotic Names with Standing in Nomenclature (LPNS)
94 (<http://www.bacterio.net/>). Phylogenetic tree based on 16S rRNA gene sequence from type strains
95 obtained from LPNS and other strains was constructed using MEGA6 [27]. The evolutionary history
96 was inferred by using the Maximum Likelihood method based on the Kimura 2-parameter model [28].
97 Initial tree(s) for the heuristic search were obtained by applying the Neighbor-Joining method to a
98 matrix of pairwise distances estimated using the Maximum Composite Likelihood (MCL) approach.
99 The tree was drawn to scale, with branch lengths measured in the number of substitutions per site.

100 Genomes publically available were retrieved from NCBI or from Integrated Microbial
101 Genomes (IMG) platform (<http://img.jgi.doe.gov/>) developed by the Joint Genome Institute, Walnut
102 Creek, CA, USA [29]. Genomes were tested for quality based on completeness (data not shown) and
103 59 have been considered for further analysis. The list of the genomes, the size and the accession
104 number are available in Table S1. After genome annotation (see below), genomes were classed as
105 methylators (including known methylators, ie., those whose methylation activity has been
106 demonstrated experimentally and putative methylators, ie., those harboring *hgcA* and *hgcB* genes
107 but which potential has never been tested) and non methylators.

108

109 *2b. Genome annotation and handing*

110 The 59 genome fasta files were processed with prokka
111 [<https://www.ncbi.nlm.nih.gov/pubmed/24642063>] version 1.12 using standard parameters. The

112 resulting protein files were clustered with orthoMCL
113 [<https://www.ncbi.nlm.nih.gov/pubmed/12952885>] version 2.0 with the following blast parameters :
114 -F 'm S' -v 100000 -b 100000 -z 541540 -e 1e-5 -m8. The generated group file was process with an
115 awk command line to count for each group the number of proteins participating in this group for
116 each genome to generate a matrix. A similarity heatmap was drawn for this matrix using the
117 pheatmap [<https://cran.r-project.org/web/packages/pheatmap/index.html>] R package. Principal
118 Coordinates Analysis (PCoA) was performed with the same matrix using MVSP software (Multi-
119 Variate Statistical Package 3.12d, Kovach Computing Services, 1985-2001, UK). A groups partitioning
120 was performed with the cascadeKM function of KMean (Vegan package, R), using ssi criterion and
121 10000 iterations.

122 Genome synteny analysis was performed with MicroScope MAGE [30]. Synteny tool provides
123 statistics about the similarity results between the selected organism using standard parameters. For
124 conserved gene clusters, e.g. synteny groups (syntons) among several bacterial genomes, all possible
125 kinds of chromosomal rearrangements were allowed (inversion, insertion/deletion). Average
126 Nucleotide Identities (ANI) calculation were carried out in IMG/ER platform using standard
127 parameters.

128 Promoters' detection were performed using the Berkeley Drosophila Genome Project Neural
129 Network Promoter Prediction tool (www.fruitfly.org/seq_tools/promoter.html), with prokaryote and
130 a minimum score of 0.7 parameters [31] and with CNNPromoter tool (Prediction of Bacterial
131 Promoters by CNN models in genomic sequences,
132 www.softberry.com/berry.phtml?topic=cnnpromoter_b&group=programs&subgroup=deeplearn),
133 using *Escherichia coli* as model [32].

134

135

136 *2c. Mercury methylation and demethylation potentials*

137 Several strains were tested for their ability to methylate inorganic mercury and demethylate
138 methylmercury under sulfate-reducing conditions. *P. hydrargyri* BerOc1 was cultivated in medium
139 described in Ranchou-Peyruse et al. [33] supplemented with lactate (20 mM) and yeast extract (0.1%)
140 at pH 7.2 and 30°C. The other strains tested in this work were obtained from the DSMZ (Deutsche
141 Sammlung von Mikroorganismen und Zellkulturen GmbH): *Desulfovibrio inopinatus* HHQ20
142 (DSM10711T); *P. piezophilus* C1TLV30 (DSM21447T), *Desulfovibrio oxyclinae* P1B (DSM11498) and
143 *Desulfovibrio longus* SEBR2582 (DSM6739). These strains were cultivated on the associated culture
144 media and conditions indicated by the DSMZ with the exception of the strain SEBR2582 which grew
145 on its isolation medium [34].

146 For the mercury biotransformation assays, each medium was inoculated with 10% (v/v) of a
147 preculture in exponential growth determined by the optical density at 600nm. The experiments were
148 performed in glass tubes (CEM, USA) sealed with (PTFE)-coated butyl stopper with 7.5 ml of culture
149 (3 replicates). Immediately after inoculation, each assay was spiked with isotopically ¹⁹⁹Hg(II)-
150 enriched inorganic mercury (10 µg.l⁻¹) and Me²⁰¹Hg-enriched methylmercury (1 µg.l⁻¹) in order to
151 determine methylation and demethylation potentials, respectively [35]. Cultures were incubated in
152 darkness, at strain optimal temperature. The incubations were stopped at the end of the exponential
153 growth by adding HNO₃ (6N, v/v) directly into the tubes.

154 At the end of the incubation period, all the mercury species (deriving from the ¹⁹⁹Hg(II) and the
155 Me²⁰¹Hg) were determined by capillary gas chromatography (Focus GC, Thermo Electron) connected
156 to an inductively coupled plasma mass spectrometry (ICPMS X7 series, Thermo Electron) according
157 the procedure described by [36]. 1mL of the culture was submitted to derivatization using sodium
158 tetraethylborate at pH 4 and then injected in the GC-ICPMS. The amount of formed and recovered
159 mercury species deriving from the enriched isotopes 199 and 201 (i.e., Me¹⁹⁹Hg, Me²⁰¹Hg,

160 199Hg(II), 201Hg(II)) after the incubation period were calculated by isotopic pattern deconvolution
161 methodology as previously described in [37]. This method allows to correct matrix effects during the
162 derivatization step for both Hg species. The recovery vary between 90 and 100% of the total amount
163 of added mercury [37]. The methylation potentials (M) were calculated by dividing the total amount
164 of Me199Hg formed by the amount of 199Hg(II) spiked. The demethylation potentials (D) were
165 obtained by dividing the amount of Me201Hg disappearing with respect to the amount of Me201Hg
166 added. At initial and final times, proteins concentrations were quantified (QuantiPro™ BCA assay
167 kit, Sigma Aldrich) in order to normalize the biotransformation rates.

168

169 *2d. Expression analysis*

170 BerOc1 cells were grown on fumarate respiration with different concentrations of inorganic
171 Hg (0 ppb, 10 ppb and 1 ppm) using the multipurpose medium supplemented with fumarate and
172 pyruvate [18] until OD600 of 0.12. Total RNA were extracted using Allprep DNA/RNA Mini kit (Qiagen)
173 and the RNA fractions were treated with DNase-Ambion Turbo DNA free (Thermofisher) at 37 °C for
174 30 min to remove DNA traces. The absence of DNA in the total RNA extracts was checked via PCR.
175 The reverse transcription (RT) was next performed using 40 units of M-MLV reverse transcriptase
176 enzyme (Invitrogen), 2.5 nM random primers, 5 µg of RNA, 200 µg dNTP and the RT reactions were
177 performed as instructed by the manufacturer. PCR were performed on cDNA samples using F-75 (5'-
178 CTGCACAGTGAAGACGAAA-3') F1 (5'-CTGCACAGTGAAGACGAAA-3') and F2 (5'-
179 TACGCCATAAAGCCGTTC-3') forward and R (5'-GTTCACGCTGTAGACGATCT-3') reverse primers.

180

181

182 3. Results and discussion

183 3a. General characteristics of *Desulfovibrio* and *Pseudodesulfovibrio* genera

184 Representatives of *Desulfovibrio* genus are found in a wide variety of anoxic and mesothermal
185 environments. Since 1895 when Beijerinck isolated the first pure strain of the *Desulfovibrio* genus,
186 new species have been regularly described. Today, this genus is phylogenetically and metabolically
187 diverse and includes 68 validate species. *Desulfovibrio vulgaris* Hildenborough has been used as a
188 model for physiology and genetics of sulfate-reducers and also for deciphering anaerobic
189 metabolisms in general (see for example <http://desulfovibriomaps.biochem.missouri.edu/>). Based on
190 16S rRNA-based phylogenetic tree (Fig. 1) two main clusters phylogenetically distant are observed.
191 The overall similarity between 16S rRNA genes is 89%. It can reach as low as 83% for pairwise
192 comparison between some species with the type strain *Desulfovibrio desulfuricans* Essex6 (type
193 species of the genus *Desulfovibrio*), indicating that *Desulfovibrio* genus includes currently species that
194 must be affiliated with other genera, even other families (16S rDNA similarity threshold considered is
195 94% for genera and 85% for families [38]. Recently, Cao and coll [9] proposed *Pseudodesulfovibrio* as
196 a new genus, mainly based on the 16S rRNA phylogeny. This new genus includes *Pseudodesulfovibrio*
197 *indicus* strain J2 [9] and *P. hydrargyri* strain BerOc1 [33]. Four other species, affiliated today with
198 *Desulfovibrio* genus: *Desulfovibrio profundus*, *Desulfovibrio piezophilus*, *Desulfovibrio aespoensis* and
199 *Desulfovibrio portus* (Fig. 1), can be revisited and considered as *Pseudodesulfovibrio* [9].

200 Today, there are many *Desulfovibrio* genomes available, most of them of high quality (data
201 not shown), and represented all through the phylogenetic tree based on the 16S rRNA gene
202 sequences (Fig. 1). We analyzed the genomes of high quality from 59 strains distributed among
203 *Desulfovibrio* and *Pseudodesulfovibrio* genera (Table S1). All those genomes have been annotated
204 with prokka [39] in order to obtain the annotation of these genomes in the same manner. The
205 genome size varied from 2.6 Mb to 5.8 Mb and a good correlation could be observed between the

206 size and the number of annotated genes (Fig. S1); *D. inopinatus* strain HHQ20 harboring the largest
207 genome and the highest number of proteins annotated. A total of 13,536 family genes has been
208 annotated and 522 were detected in the 59 genomes analyzed (Fig. 2). This core genome represents
209 only 3.8% of the genes annotated, highlighting the divergence between genomes. Two genomes (*i.e.*
210 *D. vulgaris* strain Hildenborough and *D. vulgaris* strain RCH1) are extremely similar, explaining the
211 few numbers of genes present in only one genome.

212 Recently, different studies proposed strains affiliation using genomic data (as example, [40]).
213 Genomic data available are crucial for deciphering the complexity of (*Pseudo*)*Desulfovibrio* genus,
214 and provide better tools for species affiliation that are actually identified among this genus. The PCoA
215 (Fig. 3) and clustering analyses (Fig. 4) based on the annotated genomes allows the discrimination of
216 specific groups that are the same as 16S rDNA phylogeny-based groups (Fig. 1). From the whole
217 genome dataset (Fig. 3.A), three groups are discriminated: Magneticus, Vulgaris and Desulfuricans
218 groups. This latter group includes *D. desulfuricans* strain Essex 6 (the type species of the *Desulfovibrio*
219 genus) that appears considerably distant from other *Desulfovibrio* strains, either phylogenetically
220 (based on 16S rRNA gene phylogeny), or metabolically (based on the whole genome annotation).
221 Desulfuricans/Vulgaris and Magneticus groups are separated in the two main branches of the 16S
222 rRNA based phylogenic tree. Removing these three groups from the PCoA (Fig. 3.B) allows the
223 identification of three other clusters: Pseudodesulfovibrio, Africanus and Salexigens groups. All these
224 groups appeared significantly different based on cascadeKM analysis (data not shown). The 16S rRNA
225 gene sequences and the functional analyses of the genomes (Fig. 4) provide new information in order
226 to reclassify few species of *Desulfovibrio* genus as *Pseudodesulfovibrio*. The *Pseudodesulfovibrio*
227 group includes the strain ND132, a well-known mercury methylator. This strain has been incorrectly
228 affiliated with *D. desulfuricans*, however, it is phylogenetically very close to BerOc1 and J2 by 16S
229 rRNA analysis (98.3% similarity). Nevertheless, ANI analysis as well as DNA-DNA hybridization of

230 ND132 with BerOc1 (data not shown) separates them in different species (Table 1), indicating that
231 ND132 represents a new species within the *Pseudodesulfovibrio* genus. Likewise, other strains belong
232 probably to this new genus as proposed by Cao and coll [9]: the phylogenetic tree and the high
233 percentage of genes present in synteny groups (Table 1) suggest that *D. piezophilus* strain C1TLV30
234 and *D. aespoensiis* strain Aspo-2 could be affiliated to the *Pseudodesulfovibrio* genus, even if the ANI
235 values are considerably low. In the same way, the remaining species of *Desulfovibrio* genus should be
236 subdivided into several new genera based on comparative analyses with the type strain genomes.

237

238 *3b. Genome comparison of putative mercury methylating Desulfovibrio and Pseudodesulfovibrio* 239 *strains*

240 Comparative genomics of (*Pseudo*)*Desulfovibrio* strains is an important step towards
241 understanding genomic characteristics related to methylation of mercury. In 2013, Parks et al. [17]
242 showed that mercury methylation requires the cluster of genes *hgcA* and *hgcB*. Based on the
243 presence or the absence of these two genes, we classified *Desulfovibrio* genomes in two groups.
244 Interestingly, all the seventeen strains carrying those two genes are phylogenetically located in the
245 same branch of the 16S rRNA gene tree (Fig. 1, tagged with black or white squares). Two strains carry
246 only one of the two genes: *D. piezophilus* C1TLV30T lacks *hgcA* whereas *Desulfovibrio vietnamensis*
247 G3 100T lacks *hgcB*. In addition, sequences alignment of *D. vietnamensis* G3 100T HgcA with HgcA
248 sequences from other *Desulfovibrio* revealed that the conserved motif essential for methylation
249 (NVWCAAGK, [41]) is absent, and more specifically the Cys-93 (required for Hg methylation in ND132)
250 is replaced by a Lysine (Fig. S2). This protein sequence, along with the lack of HgcB, suggests that *D.*
251 *vietnamensis* G3 100T is unable to methylate mercury. The absence of Cys-93 in *D. vietnamensis* HgcA
252 may suggest that this protein perform different function than Hg methylation. However, *D.*
253 *vietnamensis* is located in the lower branch of the phylogenetically tree, while all the others putative

254 methylators are located in the upper branch (Fig. 1). This observation might suggest an evolutionary
255 scenario. In this latter hypothesis, HgcA from *D. vietnamensis* would have lost its main function by
256 mutating the essential part of the protein, before becoming a pseudogene and then completely
257 disappear. This evolutionary process, commonly found for other genes [42], could explain why the
258 *hgcA* gene is only found in one branch on the phylogenetic tree and makes possible to imagine that
259 the mercury methylation function was widespread but may be in process of disappearing in some
260 microorganisms.

261 On the other hand, *D. piezophilus* C1TLV30 carries a *hgcB*-like gene, but lacks *hgcA* (Fig. 5).
262 Similarity and phylogenetic analyses showed that putative methylating strains contain *hgcB* gene and
263 at least one *hgcB* paralogue, named *hgcB*-like (Fig. S3). The function of these *hgcB* paralogues is still
264 unknown but are not involved in mercury methylation. Indeed, the *hgcB* deleted mutant of *D.*
265 *desulfuricans* strain ND132 [17] was unable to produce methylmercury, indicating that the second
266 copy (*i.e.* *hgcB*-like) was unable to replace *hgcB* gene in the mercury methylation process. Indeed, the
267 *hgcB*-like paralogues lack Cys-73 and Cys94-Cys-95 (Fig S3) already described as essential for mercury
268 methylation [41].

269 Except for *hgcA* and *hgcB* genes, no specific gene markers could be detected for methylating
270 bacteria. PCoA showed the methylators (Fig. 3) dispersed among the non methylators. Thorough
271 genomic comparison did not identify other genes exclusively found in Hg methylators (data not
272 shown).

273 The recently discovery of *hgcA* and *hgcB* genes in uncultured microaerophilic bacteria [8]
274 suggests that the methylation potential via these genes could be widely distributed and not restricted
275 to anaerobic microorganisms. An effort to isolate this microaerophilic bacterium and experimentally
276 demonstrate their methylation potential is important to break our perception of mercury

277 methylation that may not necessarily be exclusive to anaerobic environments. This will bring new
278 insights on mercury methylation prevalence and its evolution among microorganisms.

279 3c. Genomes' synteny on *hgcA* and *hgcB* locus

280 In most of the genomes investigated here, including *D. desulfuricans* strain N132 [17], *hgcA*
281 and *hgcB* genes are adjacent (Fig. 5). However, *D. africanus* subspecies strains Benghazi, PCS and WB
282 and *Desulfovibrio* strain L21-Syr-AB contain between *hgcA* and *hgcB* genes one ORF coding
283 respectively for a radical SAM domain protein and a putative carbon monoxide dehydrogenase. In
284 addition, more than 29 000 bp separate both genes in the genome of *D. inopinatus* strain HHQ20.

285 Genome's structure of *hgcA* and *hgcB* locus is almost identical in strains related to
286 *Pseudodesulfovibrio* strains BerOc1, ND132 and J2 (Fig. 5). *D. aespoeensis* strain Aspo-2 has the same
287 locus structure, except the four genes located downstream *hgcB* are absent (although the following
288 genes are within the synton but not shown in figure 5). For *D. oxycliniae* strain P1B the four genes
289 downstream *hgcB* are also absent, however, genes located upstream *hgcA* are found in synteny
290 elsewhere in the genome (Fig. 5). *D. piezophilus* strain C1TLV30 shows an interesting genome
291 structure at the *hgcB*-like locus. Although this gene is more similar to the *hgcB* paralogue of *P.*
292 *hydrargyri* strain BerOc1 (96% of identity), it is in synteny with BerOc1 *hgcB*. Synteny comparison
293 between these two strains revealed that there is a synton of near 52 kbp, including 62 genes in
294 BerOc1 and 52 in C1TLV30. In BerOc1, this syntonic sequence is flanked in both of its extremities by
295 *hgcB* and *hgcB*-like genes (Fig. S4 and Table S2). In the case of the strain C1TLV30, the synton is
296 flanked by *hgcB*-like gene and another gene encoding for a putative 4Fe-4S ferredoxin iron-sulfur
297 binding domain protein, different of *hgcB* and *hgcB*-like sequences (Table S2). This structure suggests
298 a putative recombination locus, with *hgcB* sequence as a recombination site, in which strain BerOc1
299 would have kept the two copies (*i.e.* *hgcB* and *hgcB*-like) whereas strain C1TLV30 (or its ancestor)

300 would have lost *hgcB* gene and harbors only *hgcB*-like gene. This hypothesis would explain why *D.*
301 *piezophilus* is the only strain in the Pseudodesulfovibrio group lacking *hgcB* (Table S1).

302 In order to decipher the effect of the different structure of *hgcA* and *hgcB* genes locus in
303 mercury methylation, we selected five model strains for mercury methylation assays. Among them,
304 only *P. hydrargyri* strain BerOc1 has been described experimentally as mercury methylator [4,18,35].
305 All the strains harboring *hgcA* and *hgcB* genes were able to perform mercury methylation (Table 2).
306 As expected, *D. piezophilus* strain C1TLV30, which only harbors *hgcB*-like, is not capable to perform
307 this process (Table 2). *D. inopinatus* strain HHQ20, where *hgcA* and *hgcB* are separated by 29 kbp,
308 showed the highest mercury methylation potential (1.32 ± 0.04 %/mg.l⁻¹ of proteins) demonstrating
309 that genomic co-localization of *hgcA* and *hgcB* does not favor mercury methylation.

310 Demethylation of MeHg assays performed simultaneously [35], showed that all the tested
311 strains were able to perform demethylation (Table 2). *D. longus* strain DSM6739 exhibited the
312 highest demethylation rates (1.51 ± 0.16 %/mg.l⁻¹ of proteins). Consequently, while *D. longus* strain
313 DSM6739 is a net MeHg demethylator with a Methylation/Demethylation rate of 0.34, *P. hydrargyri*
314 strain BerOc1 (5.57), *D. inopinatus* strain HHQ20 (7.87) and *D. oxyclinae* strain P1B (3.85) are net
315 mercury methylators.

316 *3d. Identification of a putative ArsR regulator*

317 Although *hgcA* and *hgcB* are adjacent, they are probably expressed independently. Indeed,
318 Smith and coll. [41] could detect a putative transcriptional start site right upstream *hgcB* in strain
319 ND132. *In silico* analysis in *P. hydrargyri* strain BerOc1, could not identify promoter region upstream
320 *hgcA*. However, sequence analysis of genes upstream *hgcA* (Fig. 5) identified in some strains an ORF
321 coding for the well-known transcriptional regulator ArsR that belongs to the metal-sensing
322 ArsR/SmtB family of repressors. This family of regulator are responsive to a variety of metals, such as

323 Zn, Ni and As [43]. They can also sense some forms of mercury and can be involved in *mer* operon
324 regulation [44], suggesting a putative role of ArsR in modulating the expression of *hgcA* or
325 *hgcA/hgcB*. Interestingly, the bioinformatics analysis performed in this work did not identify a
326 promoter region right upstream *hgcA* gene. The only promoter region identified so far near *hgcA* is
327 located upstream *arsR* gene suggesting that *arsR* and *hgcA* could be co-transcribed.

328 To test this hypothesis, reverse transcription-PCR (RT-PCR) was performed on total RNA
329 extracted from BerOc1 grown at the different concentrations of inorganic Hg. For this set of
330 experiment, two couple of forward primers have been used for the PCR, located either in the *arsR*
331 (F1) or in *hgcA* (F2) sequences, at 18 bp or 500 bp from the start codon of *arsR* sequence,
332 respectively. The reverse primer (R) was also located in the *hgcA*, 800 bp downstream the start codon
333 of *arsR* for both PCR (Fig. 6A). In all conditions tested, the RT-PCR performed showed PCR bands
334 corresponding to the expected size when the forward primer is located both in *hgcA* and in *arsR* (Fig.
335 6B) which demonstrate that *hgcA* and *arsR* are co-transcribed. A primer located upstream the ATG of
336 *arsR* (F-75) was used with the R primer as a control and showed no cotranscription of *hgcA* with the
337 region upstream *arsR* (data not shown). We hypothesize that as *arsR* is co-transcribed with *hgcA*,
338 ArsR could regulate the expression of *hgcA*. However, how the regulation occurs is still unknown.
339 ArsR encoding gene is probably co-transcribed with *hgcA* in other strains, but not all of them since
340 *arsR* is not always located right upstream *hgcA*. For the strains tested in our study, *D. longus*
341 SEBR2582 and *D. inopinatus* HHQ20 do not have *arsR* gene in synteny, even if several copies of
342 putative *arsR* encoding genes are found elsewhere in their genomes (data not shown). Their mercury
343 methylation potential however was comparable to BerOc1 for *D. longus* SEBR2582 and higher for *D.*
344 *inopinatus* HHQ20. Either there are different regulatory mechanisms in those strains, or there is an
345 evolutionary explanation, in which *arsR* gene has been inserted (in BerOc1) or deleted (in *D. longus*
346 and others) from *hgcAB* locus.

347 Previous transcriptomic data analysis showed that the expression of *hgcA* and *hgcB* are not
348 responsive to the presence of Hg in the growth medium [18,21,22]. Other studies have shown that
349 the presence of some metals like Zn, Cd and Cu inhibited the methylation of Hg [45–47]. In these
350 cases, if the production of MeHg is inhibited *via* a regulatory mechanism, it is very possible that *ArsR*
351 regulates the expression of *hgcA* by sensing metal other than Hg, but the response might be different
352 in different strains.

353 To summarize, *Desulfovibrio* genus includes today species that should probably be affiliated
354 with different genera. An acute affiliation of strains related to these genera is necessary to confirm
355 whether the mercury methylators are affiliated with specific genera or if they are widespread among
356 (*Pseudo*)*Desulfovibrio* species. Our results based on 16S rRNA based phylogeny and comparative
357 genome annotation identify methylators in some specific groups. However, not all the strains
358 belonging to these groups are able to perform mercury methylation. Also, the genomic structure of
359 *hgcA* and *hgcB* loci is different in the strains investigated here, and vicinity between *hgcA* and *hgcB*
360 genes does not promote higher mercury methylation potential. Understanding the phylogenetic
361 relationship of mercury methylation metabolism is essential to understand whether this metabolism
362 has a vertical inheritance. To this end, *Pseudodesulfovibrio* group is an excellent choice for future
363 studies since it contains genetically and phylogenetically close strains with different mercury
364 methylation capacities and with particular genomic structure (inverted synton in the *hgcB* locus in
365 some cases). The genomic analyses identify also *arsR* gene coding for a putative regulator located
366 upstream *hgcA*. Both genes are co-transcribed. Further experimental analysis is needed in order to
367 understand how this regulator is involved in mercury methylation.

368

369 **Conflict of interest**

370 Authors declare any conflict of interest

371 **Acknowledge**

372 This work was partially supported by the CNRS-INSU EC2CO (Biomer Project).The LABGeM
373 (CEA/Genoscope & CNRS UMR8030), the France Génomique and French Bioinformatics Institute
374 national infrastructures (funded as part of Investissement d'Avenir program managed by Agence
375 Nationale pour la Recherche, contracts ANR-10-INBS-09 and ANR-11-INBS-0013) are acknowledged
376 for support within the MicroScope annotation platform.

377

378 **References**

- 379 [1] Amos HM, Sonke JE, Obrist D, Robins N, Hagan N, Horowitz HM, et al. Observational and Modeling
380 Constraints on Global Anthropogenic Enrichment of Mercury. *Environ Sci Technol* 2015;49:4036–47.
- 381 [2] Compeau GC, Bartha R. Sulfate-reducing bacteria: principal methylators of mercury in anoxic estuarine
382 sediment. *Appl Environ Microbiol* 1985;50:498–502.
- 383 [3] Gilmour CC, Podar M, Bullock AL, Graham AM, Brown S, Somenahally AC, et al. Mercury methylation by
384 novel microorganisms from new environments. *Environ Sci Technol* 2013; 47:11810-20.
- 385 [4] Ranchou-Peyruse M, Monperrus M, Bridou R, Duran R, Amouroux D, Salvado JC, et al. Overview of
386 mercury methylation capacities among anaerobic bacteria including representatives of the sulphate-
387 reducers: implications for environmental studies. *Geomicrobiol J* 2009;26:1–8.
- 388 [5] Fleming EJ, Mack EE, Green PG, Nelson DC. Mercury methylation from unexpected sources: molybdate-
389 inhibited freshwater sediments and an iron-reducing bacterium. *Appl Environ Microbiol* 2006;72:457–64.
- 390 [6] Achá D, Hintelmann H, Pabón CA. Sulfate-reducing Bacteria and Mercury Methylation in the Water
391 Column of the Lake 658 of the Experimental Lake Area. *Geomicrobiol J* 2012;29:667–674.
- 392 [7] Gentès S, Monperrus M, Legeay A, Maury-Brachet R, Davail S, André JM, et al. Incidence of invasive
393 macrophytes on methylmercury budget in temperate lakes: Central role of bacterial periphytic
394 communities. *Environ Pollut* 2013;172:116–23.
- 395 [8] Gionfriddo CM, Tate MT, Wick RR, Schultz MB, Zemla A, Thelen MP, et al. Microbial mercury methylation
396 in Antarctic sea ice. *Nat Microbiol* 2016;1:16127.
- 397 [9] Cao J, Gayet N, Zeng X, Shao Z, Jebbar M, Alain K. *Pseudodesulfovibrio indicus* gen. nov., sp. nov., a
398 piezophilic sulfate-reducing bacterium from the Indian Ocean and reclassification of four species of the
399 genus *Desulfovibrio*. *Int J Syst Evol Microbiol* 2016;66:3904–11.
- 400 [10] Euzéby JP. List of Bacterial Names with Standing in Nomenclature: a folder available on the Internet. *Int J*
401 *Syst Bacteriol* 1997;47:590–2.
- 402 [11] Muyzer G, Stams AJM. The ecology and biotechnology of sulphate-reducing bacteria. *Nat Rev Microbiol*
403 2008;6:441–454.
- 404 [12] Pedrero Z, Bridou R, Mounicou S, Guyoneaud R, Monperrus M, Amouroux D. Transformation,
405 Localization, and Biomolecular Binding of Hg Species at Subcellular Level in Methylating and
406 Nonmethylating Sulfate-Reducing Bacteria. *Environ Sci Technol* 2012;46:11744–51.
- 407 [13] Perrot V, Bridou R, Pedrero Z, Guyoneaud R, Monperrus M, Amouroux D. Identical Hg Isotope Mass
408 Dependent Fractionation Signature during Methylation by Sulfate-Reducing Bacteria in Sulfate and
409 Sulfate-Free Environment. *Environ Sci Technol* 2015;49:1365–73.
- 410 [14] Graham AM, Bullock AL, Maizel AC, Elias DA, Gilmour CC. Detailed Assessment of the Kinetics of Hg-Cell
411 Association, Hg Methylation, and Methylmercury Degradation in Several *Desulfovibrio* Species. *Appl*
412 *Environ Microbiol* 2012;78:7337.
- 413 [15] Schaefer JK, Rocks SS, Zheng W, Liang L, Gu B, Morel FMM. Active transport, substrate specificity, and
414 methylation of Hg(II) in anaerobic bacteria. *Proc Natl Acad Sci* 2011;108:8714–9.
- 415 [16] An J, Zhang L, Lu X, Pelletier DA, Pierce EM, Johs A, et al. Mercury Uptake by *Desulfovibrio desulfuricans*
416 ND132: Passive or Active? *Environ Sci Technol* 2019;53:6264–72.
- 417 [17] Parks JM, Johs A, Podar M, Bridou R, Hurt RA, Smith SD, et al. The genetic basis for bacterial mercury
418 methylation. *Science* 2013;339:1332–5.
- 419 [18] Goñi-Urriza M, Corsellis Y, Lancelleur L, Tessier E, Gury J, Monperrus M, et al. Relationships between
420 bacterial energetic metabolism, mercury methylation potential, and *hgcA/hgcB* gene expression in
421 *Desulfovibrio dechloroacetivorans* BerOc1. *Environ Sci Pollut Res Int* 2015;22:13764–71.
- 422 [19] Date SS, Parks JM, Rush KW, Wall JD, Ragsdale SW, Johs A. Kinetics of enzymatic mercury methylation at
423 nanomolar concentrations catalyzed by HgcAB. *BioRxiv* 2019:510180.
- 424 [20] Truong H-YT, Chen Y-W, Saleh M, Nehzati S, George GN, Pickering IJ, et al. Proteomics of *Desulfovibrio*
425 *desulfuricans* and X-ray absorption spectroscopy to investigate mercury methylation in the presence of
426 selenium. *Metallomics* 2014;6:465–75.

- 427 [21] Qian C, Chen H, Johs A, Lu X, An J, Pierce EM, et al. Quantitative Proteomic Analysis of Biological
428 Processes and Responses of the Bacterium *Desulfovibrio desulfuricans* ND132 upon Deletion of Its
429 Mercury Methylation Genes. *PROTEOMICS* 2018;18:1700479.
- 430 [22] Gilmour CC, Elias DA, Kucken AM, Brown SD, Palumbo AV, Schadt CW, et al. Sulfate-Reducing Bacterium
431 *Desulfovibrio desulfuricans* ND132 as a Model for Understanding Bacterial Mercury Methylation. *Appl*
432 *Environ Microbiol* 2011;77:3938–51.
- 433 [23] Liu Y-R, Lu X, Zhao L, An J, He J-Z, Pierce EM, et al. Effects of Cellular Sorption on Mercury Bioavailability
434 and Methylmercury Production by *Desulfovibrio desulfuricans* ND132. *Environ Sci Technol*
435 2016;50:13335–41.
- 436 [24] Moreau JW, Gionfriddo CM, Krabbenhoft DP, Ogorek JM, DeWild JF, Aiken GR, et al. The Effect of Natural
437 Organic Matter on Mercury Methylation by *Desulfohalobus propionicus* 1pr3. *Front Microbiol* 2015;6.
- 438 [25] Hsu-Kim H, Kucharzyk KH, Zhang T, Deshusses MA. Mechanisms regulating mercury bioavailability for
439 methylating microorganisms in the aquatic environment: a critical review. *Environ Sci Technol*
440 2013;47:2441–56.
- 441 [26] Lin TY, Kampalath RA, Lin C-C, Zhang M, Chavarria K, Lacson J, et al. Investigation of mercury methylation
442 pathways in biofilm versus planktonic cultures of *Desulfovibrio desulfuricans*. *Environ Sci Technol*
443 2013;47:5695–702.
- 444 [27] Tamura K, Stecher G, Peterson D, Filipinski A, Kumar S. MEGA6: Molecular Evolutionary Genetics Analysis
445 Version 6.0. *Mol Biol Evol* 2013;30:2725–9.
- 446 [28] Kimura M. A simple method for estimating evolutionary rates of base substitutions through comparative
447 studies of nucleotide sequences. *J Mol Evol* 1980;16:111–20.
- 448 [29] Markowitz VM, Chen I-MA, Palaniappan K, Chu K, Szeto E, Grechkin Y, et al. IMG: the Integrated
449 Microbial Genomes database and comparative analysis system. *Nucleic Acids Res* 2012;40:D115-122.
- 450 [30] Vallenet D, Calteau A, Cruveiller S, Gachet M, Lajus A, Josso A, et al. MicroScope in 2017: an expanding
451 and evolving integrated resource for community expertise of microbial genomes. *Nucleic Acids Res*
452 2016;45:D517–28.
- 453 [31] Reese MG. Application of a time-delay neural network to promoter annotation in the *Drosophila*
454 *melanogaster* genome. *Comput Chem* 2001;26:51–6.
- 455 [32] Umarov RK, Solovyev VV. Recognition of prokaryotic and eukaryotic promoters using convolutional deep
456 learning neural networks. *PLoS One* 2017;12:e0171410–e0171410. doi:10.1371/journal.pone.0171410.
- 457 [33] Ranchou-Peyruse M, Goñi-Urriza M, Guignard M, Goas M, Ranchou-Peyruse A, Guyoneaud R.
458 *Pseudodesulfovibrio hydrargyri* sp. nov., a mercury-methylating bacterium isolated from a brackish
459 sediment. *Int J Syst Evol Microbiol* 2018;68:1461–6.
- 460 [34] Magot M, Caumette P, Desperrier J, Matheron R, Dauga C, Grimont F, et al. *Desulfovibrio longus* sp. nov.,
461 a sulfate-reducing bacterium isolated from an oil-producing well. *Int J Syst Bacteriol* 1992;42:398–403.
- 462 [35] Bridou R, Monperrus M, Gonzalez PR, Guyoneaud R, Amouroux D. Simultaneous determination of
463 mercury methylation and demethylation capacities of various sulfate-reducing bacteria using species-
464 specific isotopic tracers. *Environ Toxicol Chem* 2011;30:337–44.
- 465 [36] Monperrus M, Tessier E, Veschambre S, Amouroux D, Donard O. Simultaneous speciation of mercury and
466 butyltin compounds in natural waters and snow by propylation and species-specific isotope dilution mass
467 spectrometry analysis. *Anal Bioanal Chem* 2005;381:854–62.
- 468 [37] Rodriguez-Gonzalez P, Bouchet S, Monperrus M, Tessier E, Amouroux D. In situ experiments for element
469 species-specific environmental reactivity of tin and mercury compounds using isotopic tracers and
470 multiple linear regression. *Environ Sci Pollut Res* 2013;20:1269–80. doi:10.1007/s11356-012-1019-5.
- 471 [38] Konstantinidis KT, Tiedje JM. Towards a Genome-Based Taxonomy for Prokaryotes. *J Bacteriol*
472 2005;187:6258.
- 473 [39] Seemann T. Prokka: rapid prokaryotic genome annotation. *Bioinformatics* 2014;30:2068–9.
- 474 [40] Sangal V, Goodfellow M, Jones AL, Schwalbe EC, Blom J, Hoskisson PA, et al. Next-generation
475 systematics: An innovative approach to resolve the structure of complex prokaryotic taxa. *Sci Rep*
476 2016;6.

- 477 [41] Smith SD, Bridou R, Johs A, Parks JM, Elias DA, Hurt RA, et al. Site-directed mutagenesis of HgcA and HgcB
478 reveals amino acid residues important for mercury methylation. *Appl Environ Microbiol* 2015;81:3205–
479 17.
- 480 [42] Darmon E, Leach DRF. Bacterial genome instability. *Microbiol Mol Biol Rev MMBR* 2014;78:1–39.
- 481 [43] Saha RP, Samanta S, Patra S, Sarkar D, Saha A, Singh MK. Metal homeostasis in bacteria: the role of
482 ArsR/SmtB family of transcriptional repressors in combating varying metal concentrations in the
483 environment. *BioMetals* 2017;30:459–503.
- 484 [44] Boyd ES, Barkay T. The mercury resistance operon: from an origin in a geothermal environment to an
485 efficient detoxification machine. *Front Microbiol* 2012;3:349.
- 486 [45] Lin H, Morrell-Falvey JL, Rao B, Liang L, Gu B. Coupled Mercury–Cell Sorption, Reduction, and Oxidation
487 on Methylmercury Production by *Geobacter sulfurreducens* PCA. *Environ Sci Technol* 2014;48:11969–76.
- 488 [46] Schaefer JK, Szczuka A, Morel FMM. Effect of Divalent Metals on Hg(II) Uptake and Methylation by
489 Bacteria. *Environ Sci Technol* 2014;48:3007–13.
- 490 [47] Lu X, Johs A, Zhao L, Wang L, Pierce EM, Gu B. Nanomolar Copper Enhances Mercury Methylation by
491 *Desulfovibrio desulfuricans* ND132. *Environ Sci Technol Lett* 2018;5:372–6.
- 492
- 493
- 494

495 **Figure captions**

496 Figure 1: 16S rRNA based phylogeny of strains identified as *Desulfovibrio* or *Pseudodesulfovibrio*. The
 497 tree with the highest log likelihood (-13240.5073) is shown. The percentage of trees in which the
 498 associated taxa clustered together is shown next to the branches. The analysis involved 93 nucleotide
 499 sequences. All positions containing gaps and missing data were eliminated. There were a total of 814
 500 positions in the final dataset. Dot: strains with available sequenced genome; black square: mercury
 501 methylating strains (experimentally validated); white square: putative mercury methylating strains
 502 (harboring *hgcA* and *hgcB* genes); black star: strain unable to methylate mercury (experimentally
 503 validated); black pentagon: strain harboring an *hgcA*-like gene. In this work, the diversity of these two
 504 genera is divided into 6 different groups: Pseudodesulfovibrio group, Salexigens group, Africanus
 505 group, Magneticus group, Vulgaris group and Desulfuricans group. The arrow shows *Desulfovibrio*
 506 *desulfuricans* subspecies *desulfuricans* strain Essex6^T, the type strain of *Desulfovibrio desulfuricans*,
 507 which is the species type of *Desulfovibrio* genus.

508 Figure 2. Frequency of genes within the 59 analyzed (*Pseudo*)*Desulfovibrio* genomes. Genes present
 509 in only one genome are shown in the left extremity of the x-axis while genes founds in all the 59
 510 genomes (core genome, 522 genes representing 3.85% of the pangenome) are shown at the far right
 511 end.

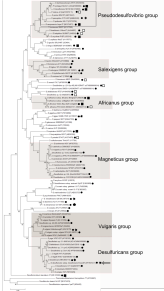
512
 513 Fig 3. Functional comparison (Principal Coordinates Analysis, Euclidian distance) based on prokka
 514 annotation of *Desulfovibrio* and *Pseudodesulfovibrio* genomes. A) Whole genome dataset; B) Dataset
 515 excluding Magneticus, Vulgaris and Desulfuricans groups; C) Dataset excluding Magneticus, Vulgaris
 516 and Desulfuricans, Africanus and Salexigens groups. Genomes related to *Pseudodesulfovibrio* are
 517 highlighted in C.

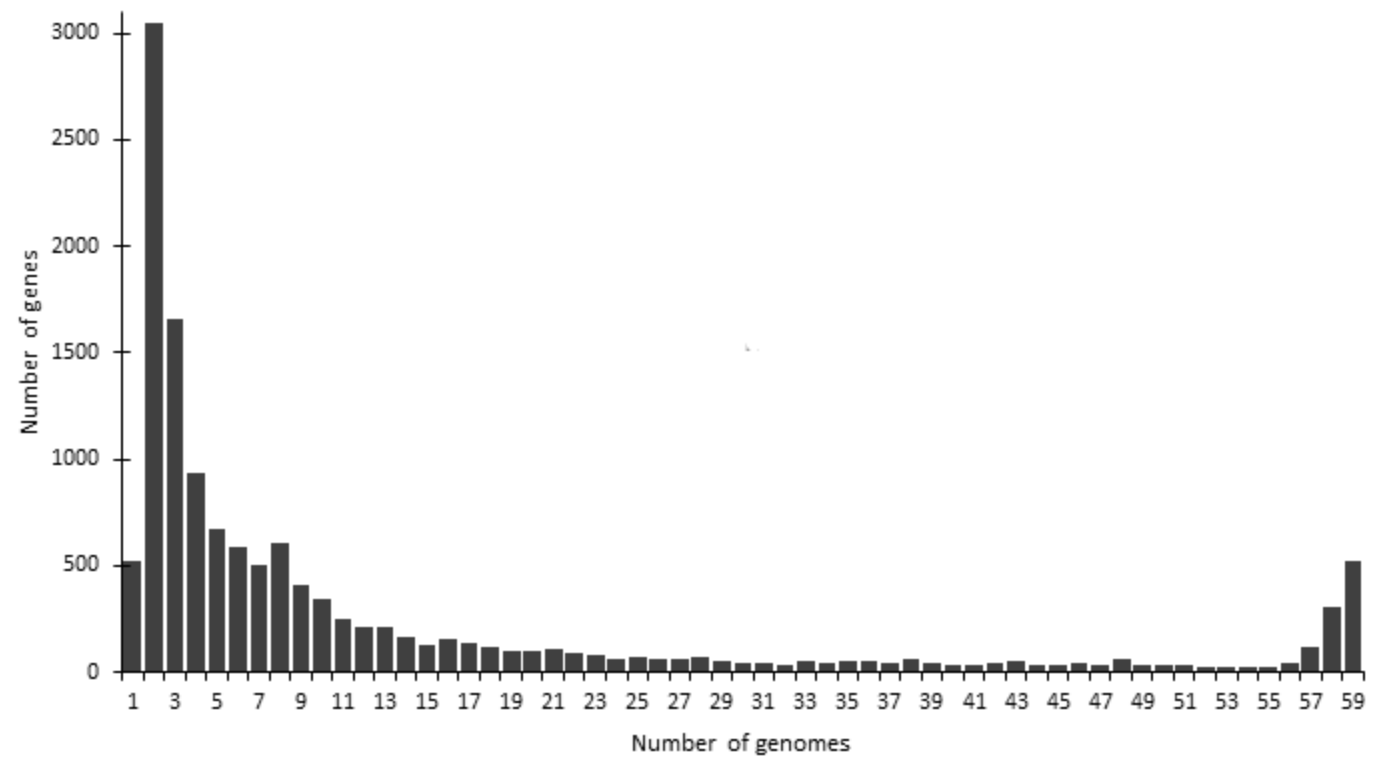
518 Fig. 4 Heatmap showing a pairwise functional comparison. Genomes' clustering is also shown. Groups
 519 of genomes determined in phylogenetic tree (Fig. 1) and in PCoA (Fig. 2) are highlighted. For genomic
 520 code of each strain, see Table S1.

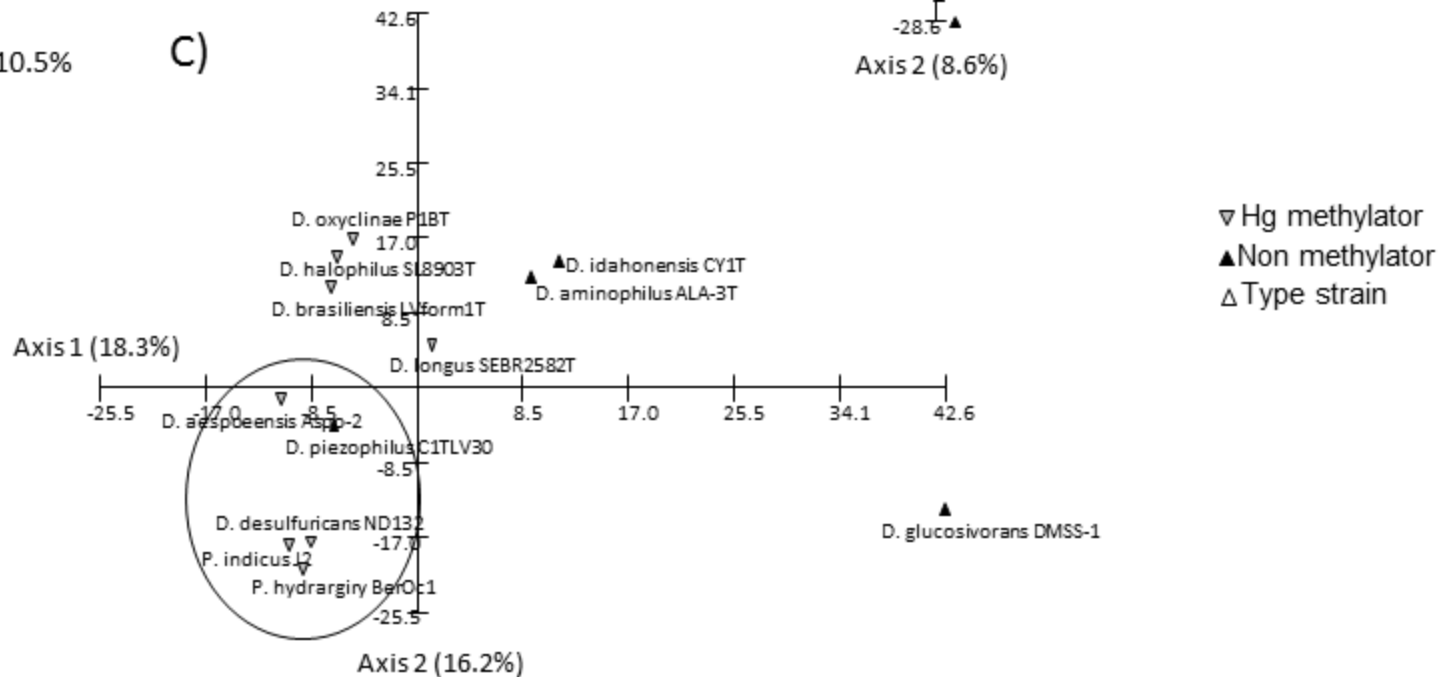
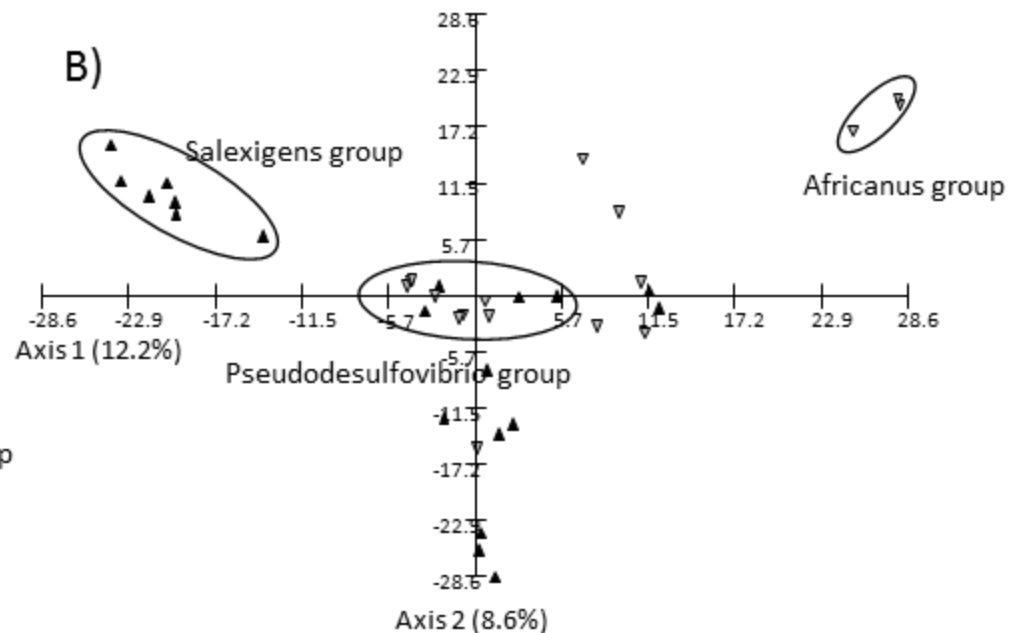
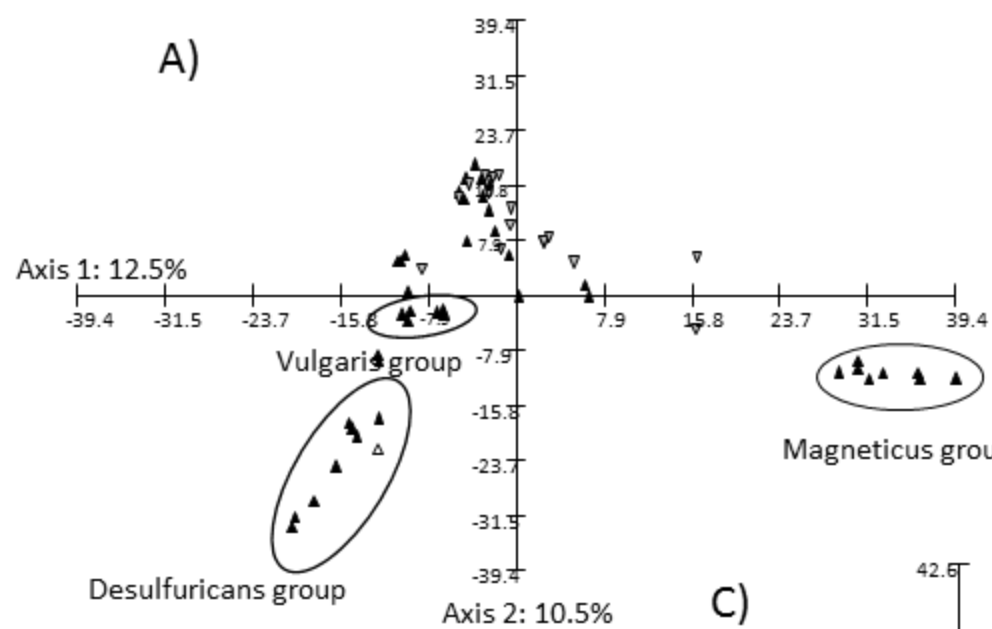
521 Fig 5. Synteny at *hgcA* and *hgcB* loci for different strains among *Desulfovibrio* and
 522 *Pseudodesulfovibrio* genera and *Desulfomicrobium baculatum* strain X. Upper panel: *Desulfovibrio* or
 523 *Pseudodesulfovibrio* strains harboring *hgcA* and *hgcB* genes. Middle panel: *Desulfovibrio* strains
 524 lacking *hgcA* gene. Lower panel: Genomic structure of *hgcA* and *hgcB* loci in *D. baculatum* strain X.
 525 Strains labeled with an asterisk are able to methylate mercury (experimentally validated). Strain
 526 labeled with a diamond is unable to perform mercury methylation (experimentally validated). Genes
 527 in dotted arrows: *hgcA* and *hgcB*. Genes in black dotted arrows: *arsR* gene. Gene in black arrow:
 528 *hgcA*-like gene in *D. vietnamensis*. Gene in hatched arrow: *hgcB*-like gene in *D. piezophilus*. Genes in
 529 grey arrows: genes found in synteny distantly located from *hgcAB* locus.

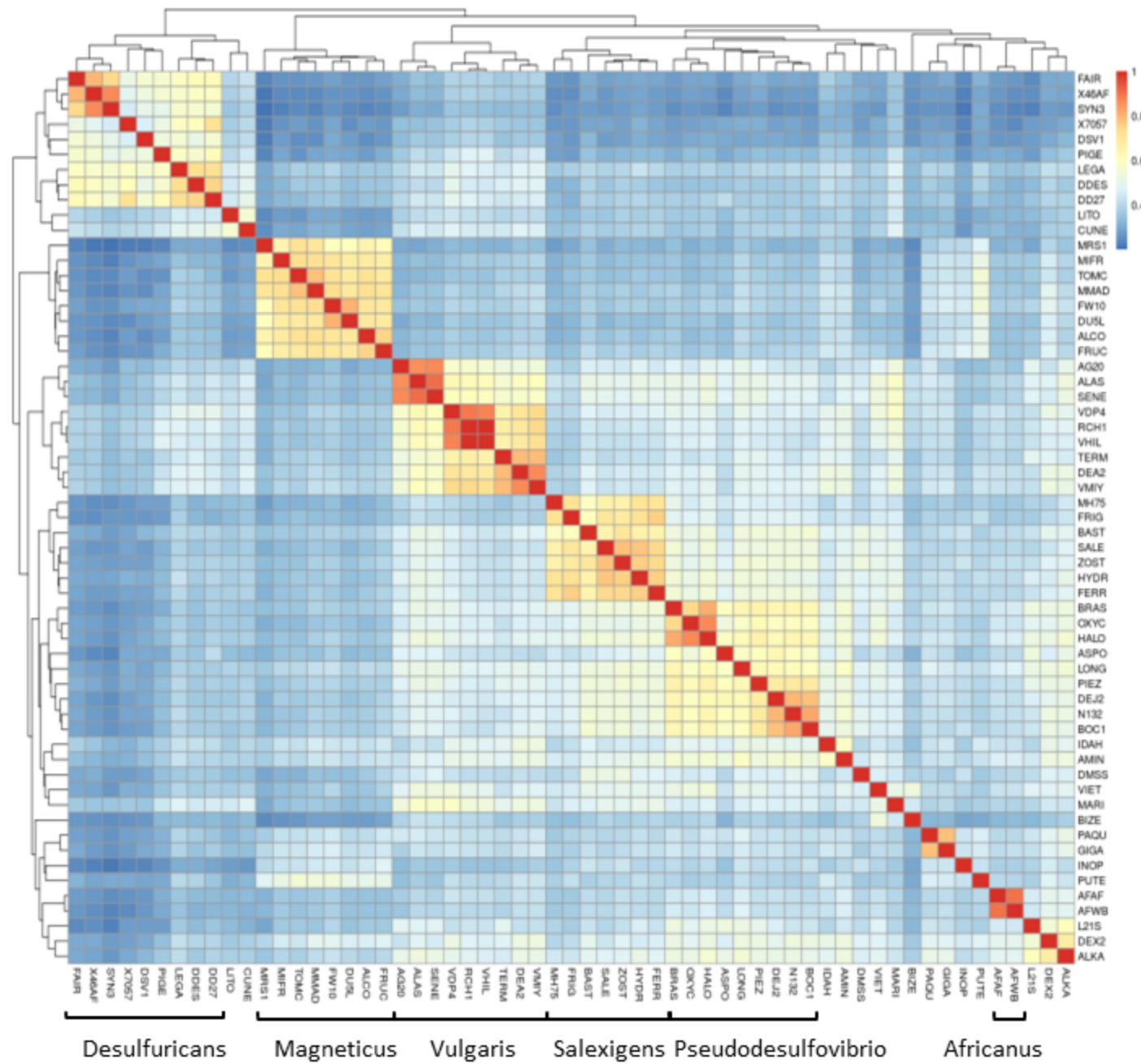
530 Fig. 6: Reverse transcription-PCR (RT-PCR) performed on total RNA extracted from BerOc1 grown at
 531 the different concentrations of inorganic Hg. A- Position of the primers used for the RT-PCR. The
 532 forward primer F1 is located 18 bp downstream the ATG of *arsR* gene, F2 is located in *hgcA*, 500 bp
 533 downstream of ATG of *arsR*, F-75 is located 75 bp upstream the ATG of *arsR* gene, and the reverse
 534 primers R is located 800 pb downstream the same ATG. B- Results of the RT-PCR performed with
 535 primers F1-R (~ 330pb) and F2-R (~ 800 bp).M: ladder, C: negative control with no addition of cDNA,
 536 C+: positive control of the PCR using the genomic DNA of BerOc1 as template. Lane 1, 2, 3 correspond
 537 to the RT-PCR performed using RNA extract from BerOc1 cells grown in the absence and in the
 538 presence of 10 ppb and 1 ppm of inorganic Hg, respectively

539









Desulfuricans

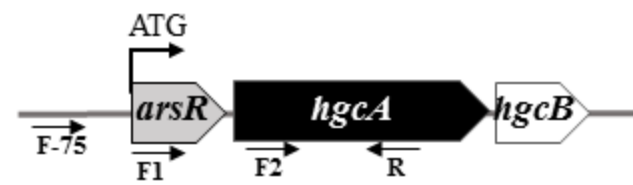
Magneticus

Vulgaris

Saalexigens Pseudodesulfovibrio

Africanus

A



B

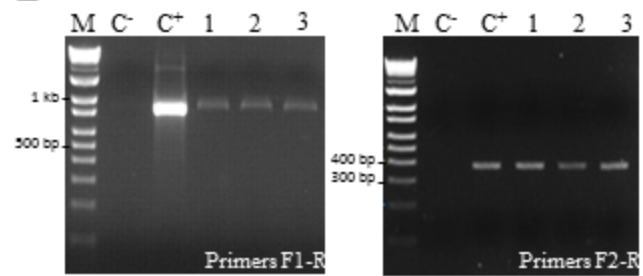


Table 1. Average Nucleotide Identity (ANI) and percentage of genes found in synteny related to *P. hydrargyri* strain BerOc1.

| Species | Strain | Methylator | Type strain | Genome size (kbp) | ANI related to BerOc1(a) | % of genes in synteny (related to BerOc1) (a) |
|--------------------------|------------|------------|-------------|----------------------|-----------------------------|--|
| <i>P. hydrargyri</i> | BerOc1 | Yes | No | 4081 | 100 | 100 |
| <i>D. desulfuricans</i> | ND132 | Yes | No | 3858 | 89 | 73,13 |
| <i>P. indicus</i> | J2 | Putative | Yes | 3966 | 84,58 | 71,88 |
| <i>D. aespoeensis</i> | Aspo -2 | Putative | Yes | 3629 | 78,22 | 58,48 |
| <i>D. longus</i> | SEBR2582 | Yes (b) | Yes | 3703 | 73,57 | 49,33 |
| <i>D. halophilus</i> | SL8903 | Putative | Yes | 3444 | 73,55 | ND |
| <i>D. oxyclinae</i> | P1B | Yes (b) | Yes | 3327 | 73,12 | 50,84 |
| <i>D. piezophilus</i> | C1TLV30 | No (b) | Yes | 3644 | 72,74 | 61,48 |
| <i>D. alkalitolerans</i> | RT2 | Putative | Yes | 3202 | 71,3 | 38,81 |
| <i>D. africanus</i> | Walvis Bay | No | Yes | 4200 | 71,08 | 39 |
| <i>D. desulfuricans</i> | Essex6 | No | Yes (d) | 3392 | 69,35 | 27,87 |
| <i>D. salexigens</i> | DSM2638 | No | Yes | 4289 | 69,27 | 45,57 |
| <i>D. inopinatus</i> | HHQ20 | Yes (b) | Yes | 5767 | 68,98 | 40,13 |
| <i>D. hydrothermalis</i> | AM13 | No | Yes | 3703 | 68,35 | 42,37 |

a) Based on 4097 CDS (including 6 CDS manually annotated as artefact.)

b) Experimentally validated in the present study

c) Genus type strain

Table 2: Potential of methyl mercury production (M% of methyl mercury production/ mg.l⁻¹ of total proteins) and methylmercury demethylation (D% of methyl mercury demethylation/ mg.l⁻¹ of total proteins) of selected *Desulfovibrio* and *Pseudodesulfovibrio* strains. M/D: ratio of methylation and demethylation potentials.

| | M(%)/mg.l ⁻¹ prot | SD | D(%)/mg.l ⁻¹ prot | SD | M/D |
|-----------------------|------------------------------|------|------------------------------|------|------|
| <i>P. hydrargyri</i> | 0.57 | 0.01 | 0.10 | 0.02 | 5.57 |
| <i>D. piezophilus</i> | 0.01 | 0.01 | 0.11 | 0.10 | 0.09 |
| <i>D. longus</i> | 0.51 | 0.01 | 1.51 | 0.16 | 0.34 |
| <i>D. inopinatus</i> | 1.32 | 0.04 | 0.17 | 0.04 | 7.87 |
| <i>D. oxycliniae</i> | 0.80 | 0.02 | 0.21 | 0.07 | 3.85 |